Stem Cell Research 53 (2021) 102250

Contents lists available at ScienceDirect

Stem Cell Research

journal homepage: www.elsevier.com/locate/scr

LncRNA Mrhl orchestrates differentiation programs in mouse embryonic stem cells through chromatin mediated regulation

Debosree Pal [a,1], C.V. Neha [a,2], Utsa Bhaduri [a,3], Zenia Zenia [a,4], Sangeeta Dutta [a], Subbulakshmi Chidambaram [b], M.R.S. Rao [a,*]

[a] Molecular Biology and Genetics Unit, Jawaharlal Nehru Centre for Advanced Scientific Research, Jakkur P. O., Bangalore 560064, India
[b] Department of Biochemistry and Molecular Biology, Pondicherry University, Puducherry 605014, India

ARTICLE INFO

Keywords:
Mrhl
LncRNA
Embryonic stem cells
Transcriptome
Chromatin
Differentiation

ABSTRACT

Long non-coding RNAs (lncRNAs) have been well-established to act as regulators and mediators of development and cell fate specification programs. LncRNA Mrhl (meiotic recombination hotspot locus) has been shown to act in a negative feedback loop with WNT signaling to regulate male germ cell meiotic commitment. In our current study, we have addressed the role of Mrhl in development and differentiation using mouse embryonic stem cells (mESCs) as our model system of study. Mrhl is a nuclear-localized, chromatin-bound lncRNA with moderately stable expression in mESCs. Transcriptome analyses and loss-of-function phenotype studies revealed dysregulation of developmental processes, lineage-specific transcription factors and key networks along with aberrance in specification of early lineages during differentiation of mESCs. Genome-wide chromatin occupancy studies suggest regulation of chromatin architecture at key target loci through triplex formation. Our studies thus reveal a role for lncRNA Mrhl in regulating differentiation programs in mESCs in the context of appropriate cues through chromatin-mediated responses.

Key Resources Table

Reagent or resource	Source	Identifier
Antibodies		
Anti-GAPDH	Abeomics	ABM22C5
Anti-H3	Abcam	Ab46765
Anti-β-catenin	Abcam	Ab6302
Anti-p68	Novus Biologicals	Custom-made
Anti-Laminin	Abcam	Ab
Bacterial and Virus Strains		
Sure 2	Stratagene	200152
Biological Samples		
N/A		
Chemicals, Peptides, and Recombinant Proteins		
Leukemia Inhibitory Factor	Merck-MIllipore	ESG1107

(*continued on next page*)

* Corresponding author.
E-mail address: mrsrao@jncasr.ac.in (M.R.S. Rao).
[1] Present address: Blizard Institute, Barts and the London School of Medicine and Dentistry, Queen Mary University of London, London E1 2AT, United Kingdom.
[2] Present address: Department of Cell and Developmental Biology, University of Illinois at Urbana-Champaign, Urbana, IL 61801, USA.
[3] Present address: Department of Life Sciences, University of Trieste, Trieste, Italy, and EU H2020 TRIM-NET ITN, Marie Sklodowska-Curie Actions (MSCA).
[4] Present address: Department of Tissue Morhphogenesis, Max PlanckInstitute of Molecular Biomedicine, Rontgenstr. 20, 48149, Munster, Germany.

https://doi.org/10.1016/j.scr.2021.102250
Received 20 February 2020; Received in revised form 15 January 2021; Accepted 10 February 2021
Available online 16 February 2021

(*continued*)

Reagent or resource	Source	Identifier
Trans-IT-X2	Mirus	MIR 6003
Protein A dynabeads	Thermo Fischer Scientific	10002D
Protein G dynabeads	Thermo Fischer Scientific	10004D
Critical Commercial Assays		
N/A		
Deposited Data		
Raw and analyzed data, RNA-Seq	This paper	GSE159757
Raw and analyzed data, ChIRP-Seq	This paper	To receive
GENCODE mm10 Release M17 (GRCm38.p6)	GENCODE	https://www.gencodegenes.org/mouse/release_M17.html
Experimental Models: Cell Lines		
E14TG2A	Gift from Prof. Tapas K. Kundu, JNCASR, India	
Experimental Models: Organisms/Strains		
N/A		
Oligonucleotides		
Mrhl shRNA#1: 5'GCACATACATACATACACATATATT	Arun et al. (2012)	doi: 10.1128/MCB.00006-12
Mrhl shRNA#4: 5'GGAGAAACCCTCAAAAGTATT 3'	Arun et al. (2012)	doi: 10.1128/MCB.00006-12
Mrhl ChIRP Oligo #1: 5'-AGTCAGATTACTGCTGGTCAGAACTAATAAACTCA-3'	This paper	N/A
Mrhl ChIRP Oligo #2: 5'-CTGCTTCCTTCCTGGAATCAACAATAAAGCAGTTA-3'	This paper	N/A
Mrhl ChIRP Oligo #3: 5'-ACTTCTTTCCAGTGACTGCAATTATCTTACAGAAGA-3'	This paper	N/A
Mrhl ChIRP Oligo #4:5'-TGAGTTTATTAGTTCTGACCAAGCAGTAATCTGACT-3'	This paper	N/A
Mrhl ChIRP Oligo #5:5'-TAACTGCTTTATTGTTGATTCCAGGAAGGAAGCAG-3'	This paper	N/A
Mrhl ChIRP Oligo #6:5'-TCTTCTGTAAGATAATTGCAGTCACTGGAAAGAAGT-3'	This paper	N/A
Lacz ChIRP Oligo #1:5'-CCAGTGAATCCGTAATCATG-3'	This paper	N/A
Lacz ChIRP Oligo #2:5'-TCACGACGTTGTAAAACGAC-3'	This paper	N/A
Recombinant DNA		
Plko.1-Puro-CMV-turboGFP + custom shRNA	Sigma-Aldrich	N/A
Plko.1-Puro-CMV-turboGFP + non-mammalian shRNA control	Sigma-Aldrich	SHC002
Software and Algorithms		
FastQC	Simon Andrews, Babraham Bioinformatics	https://www.bioinformatics.babraham.ac.uk/projects/fastqc/
TrimGalore (v 0.4.4)	Felix Krueger	https://www.bioinformatics.babraham.ac.uk/projects/trim_galore/
Bowtie2	Langmead and Salzberg (2012)	http://bowtie-bio.sourceforge.net/bowtie2/index.shtml
Samtools (v 1.3.1)	Li et al. (2009)	http://www.htslib.org/doc/samtools.html
Tophat	Trapnell et al. (2012)	https://ccb.jhu.edu/software/tophat/manual.shtml
Cufflinks	Trapnell et al. (2012)	https://bio.tools/cufflinks
Cuffmerge	Trapnell et al. (2012)	http://cole-trapnell-lab.github.io/cufflinks/cuffmerge/
Cuffdiff	Trapnell et al. (2012)	http://cole-trapnell-lab.github.io/cufflinks/cuffdiff/
CummeRbund	Goff et al. (2012)	https://www.bioconductor.org/packages/release/bioc/html/cummeRbund.html
PANTHER	Mi et al. (2012) and Thomas et al. (2003)	http://www.pantherdb.org/
Cluster 3.0	Eisen et al. (1998) and de Hoon et al. (2004)	http://bonsai.hgc.jp/~mdehoon/software/cluster/
Cytoscape	Shannon et al. (2003)	https://cytoscape.org/
GeneMania	Warde-Farley et al. (2010)	https://genemania.org/
JASPAR	Sandelin et al. (2004)	http://jaspar.genereg.net/
Bedtools	Quinlan and Hall. (2010)	https://bedtools.readthedocs.io/en/latest/
MEME	Bailey et al. (2009)	http://meme-suite.org/
STRING	Szklarczyk et al. (2015)	https://string-db.org/
Other		
N/A		

1. Introduction

Long non-coding RNAs (lncRNAs) are classified as non-coding RNAs > 200nt in length and they have been widely established to function through diverse mechanisms in development and disease (Akhade et al., 2017; Marchese et al., 2017). In the recent years, they have been implicated in embryonic stem cell (ESC) physiology in maintaining pluripotency (Bergmann et al., 2015; Chakraborty et al., 2017; Guttman et al., 2011; Sheik Mohamed et al., 2010; Sun et al., 2018b) as well as in regulating differentiation and cell fate specification programs (Flynn and Chang, 2014; Klattenhoff et al., 2013; Ulitsky et al., 2011). Some of these lncRNAs perform multiple roles as a function of the cellular contexts and interaction partners. LncRNA Gomafu/Miat/Rncr2 is involved in maintaining pluripotency of mouse ESCs (mESCs) (Sheik Mohamed et al., 2010), specification of the oligodendrocyte lineage in neural stem cells (Mercer et al., 2010) and osteogenic lineage differentiation in adipose-derived stem cells (Jin et al., 2017). LncRNA Tuna has been implicated in maintaining pluripotency of mESCs as well as their differentiation into the neural lineage (Lin et al., 2014). LncRNA Tsx has also been shown to be involved in the maintenance of mESCs, pachytene spermatocytes in testes and regulation of cognition and behaviour in mice (Anguera et al., 2011). These examples highlight the diversity and context-dependant regulatory functions of lncRNAs in stem cell physiology and development and it demands further investigations of their

roles in these processes.

LncRNA Mrhl (meiotic recombination hotspot locus) has been studied extensively in the context of male germ cell meiotic commitment. It is a 2.4 kb long, sense, intronic and single-exonic lncRNA, encoded within the 15th intron of the *Phkb* gene in mouse (Nishant et al., 2004) and is syntenically conserved in humans (Fatima et al., 2019). It has been shown to act in a negative feedback loop with WNT signaling in association with its interaction partner p68 to regulate meiotic progression of type B spermatogonial cells through regulation of *Sox8* at the chromatin level. (Akhade et al., 2016; Arun et al., 2012) These studies suggest an intricate network of Mrhl and associated proteins acting to orchestrate the process of male germ cell meiosis.

In purview of lncRNAs as context-dependent regulators of developmental phenomena, we have addressed the role of lncRNA Mrhl in mouse ESCs (mESCs) to understand its role in development and differentiation. We demonstrate through transcriptome studies that depletion of Mrhl in mESCs leads to dysregulation of >1000 genes with major perturbation of developmental processes and genes including lineage-specific transcription factors (TFs) and cell adhesion and receptor activity related genes. mESCs with stable knockdown of Mrhl displayed aberrance in specification of ectoderm, mesoderm and lineages with no changes in the pluripotency status of the cells, consistent with our transcriptome data. Genome-wide chromatin occupancy studies showed Mrhl to be associated with ~22,000 loci. We further found key developmental TFs such as RUNX2, POU3F2 and FOXP2 to be directly regulated by Mrhl at the chromatin level possibly through RNA-DNA-DNA triplex formation. Our study delineates lncRNA Mrhl as a chromatin regulator of cellular differentiation and development genes in mESCs, probably acting to maintain the cells in a more primed state, readily responsive to appropriate differentiation cues.

2. Materials and methods

2.1. Cell lines, plasmids and reagents

E14TG2a feeder independent mESC line was a kind gift from Prof. Tapas K. Kundu's lab (JNCASR, India). mESCs were maintained on 0.2% gelatin coated dishes with ESGRO (Merck Millipore).

The antibodies used in this study are as follows: Anti-GAPDH (Abeomics, ABM22C5), anti-H3 (Abcam, ab46765), anti β-CATENIN (Abcam), anti p68 (Novus Biologicals) and anti-LAMININ (ab11575).

Scrambled and Mrhl shRNA plasmids 1, 2, 3 and 4 were custom made from Sigma in the pLKO.1-Puro-CMV-tGFP vector backbone. The sequences of the shRNAs are as follows:

Mrhl shRNA#1: 5′GCACATACATACATACACATATATT 3′, Mrhl shRNA#2:5′GTGAAATGACTGTGCTTTATT 3′, Mrhl shRNA#3: 5′CAAGTTGACTGCTGATTTATT 3′, Mrhl shRNA#4: 5′GGAGAAACCCTCAAAAGTATT 3′.

All fine chemicals were obtained from Sigma (unless otherwise mentioned), gelatin was obtained from Himedia and FBS was obtained from Gibco (Performance Plus, US Origin).

2.2. Cell culture protocols

For embryoid body (EB) differentiation, 2.5×10^5 E14TG2a cells were plated onto 35 mm bacteriological grade dishes in EB differentiation medium containing DMEM, 10% FBS, 0.1 mM β-mercaptoethanol and 1X penicillin-streptomycin. Medium for EBs was changed on every alternate day. EBs were harvested by gravity precipitation at different time points and processed further for RNA extraction using TRIZol. All transfections for E14TG2a cells were performed using Trans IT-X2 reagent (Mirus, MIR 6003) as per the manufacturer's protocol. For transient knockdown analysis, cells were harvested 48 h post-transfection. Transfections for HEK293T cells were performed using Lipofectamine 2000 (Thermo Fisher Scientific) as per the manufacturer's protocol. For measurement of half-life of Mrhl, E14TG2a cells were treated with 10 μM actinomycin D (Sigma, A9415).

2.3. Generation of stable knockdown lines

Stable mESC knockdown lines for Mrhl were generated in E14TG2a cells as per the protocol of Pijnappel et al. (2013) with some modifications. Viral particles were generated in HEK293T cells by transfection of 5 μg scrambled or Mrhl shRNA plasmids, 2.5 μg pSPAX2, 1.75 μg pVSVG and 0.75 μg pRev. The media containing viral particles was harvested 48 h after transfection. Fresh mESC medium was added and harvested after an additional 24 h to collect second round of viral particles. The viral supernatant mixed with 8 μg/ml DEAE-dextran and 1000 units/ml ESGRO was added directly to the E14TG2a cells. Transduction was performed for 24 h with the first round of viral particles and an additional 24 h with the second round of viral particles. The transduced cells were then subjected to puromycin selection (1.5 μg/ml puromycin) for a week.

2.4. RNA fluorescent in situ hybridization (FISH) and immunofluorescence (IF)

RNA FISH followed by IF was performed as per the protocol of de Planell-Saguer et al. (2010) with minor modifications. The probes used for RNA FISH studies were Cy5 labelled locked nucleic acid probes procured from Exiqon (reported in Arun et al. (2012)). For FISH, samples were blocked in prehybridization buffer for 40 min at 50 °C. Hybridization was performed with prewarmed hybridization buffer for 1 h at 50 °C. After hybridization, slides were washed four times for 6 min each with wash buffer I at 50 °C followed by two washes with wash buffer II for 6 min each at 50 °C. The samples were then washed with wash buffer III once for 5 min at 50 °C followed by one wash with 1X PBS at room temperature. For tissue sections, all washes were performed as mentioned above with a time of 4 min for buffers I-III.

2.5. Cell fractionation

Approximately 5–10 million cells were lysed using lysis buffer (0.8 M sucrose, 150 mM KCl, 5 mM $MgCl_2$, 6 mM β-mercaptoethanol and 0.5% NP-40) supplemented with 75 units/ml RNAse inhibitor (Thermo Fisher Scientific) and 1X mammalian protease inhibitor cocktail [mPIC, (Roche)] and centrifuged at 10,000*g* for 5 min at 4 °C. The supernatant or pellet was taken for RNA or protein extraction as described later.

2.6. Sub-nuclear fractionation

Approximately 10 million cells were lysed with hypotonic lysis buffer (10 mM Tris-HCl pH 7.5, 10 mM NaCl, 3 mM $MgCl_2$, 0.3% v/v NP-40 and 10% v/v/ glycerol) supplemented with RNAse inhibitor and mPIC and centrifuged at 1000*g* for 5 min at 4 °C. The nuclear pellet was washed twice with hypotonic lysis buffer, resuspended in modified Wuarin-Schibler buffer (10 mM Tris-HCl pH 7.0, 4 mM EDTA, 300 mM NaCl, 1 M urea and 1% NP-40) supplemented with RNAse inhibitor and mPIC and vortexed for 10 min. Nucleoplasmic and chromatin fractions were separated by centrifugation at 1000*g* for 5 min at 4 °C. The chromatin pellet was resuspended in sonication buffer (20 mM Tris-HCl pH 7.5, 150 mM NaCl, 3 mM $MgCl_2$, 0.5 mM PMSF, 75 units/ml RNAse inhibitor) and sonicated for 10 min. The resultant nucleoplasmic and chromatin fractions were then subjected to RNA or protein extraction as described later.

2.7. p68 IP

Cells were lysed in hypotonic lysis buffer (10 mM Tris-HCl pH 7.5, 10 mM NaCl, 3 mM $MgCl_2$, 0.3% NP-40, 10% glycerol) supplemented with RNase inhibitor, mPIC and 1 mM PMSF. Nuclei were pelleted down at 1200 g for 10 min at 4 °C and subsequently lysed in nuclear lysis

buffer (150 mM KCl, 25 mM Tris pH 7.4, 5 mM EDTA, 0.5% NP-40) supplemented with RNase inhibitor, mPIC and PMSF. To 1 mg of the supernatant nuclear fraction containing proteins, 7 μg of either pre-immune serum or p68 antibody was added and incubated overnight at 4 °C. Next day, the fraction was incubated with protein A dynabeads for 3 h at 4 °C. The beads were washed with wash buffer (20 mM Tris-HCl pH 7.4, 2 mM $MgCl_2$, 10 mM KCl, 150 mM NaCl, 10% glycerol, 0.2% NP-40) supplemented with RNase inhibitor, mPIC and PMSF. Subsequently, the beads were washed twice with wash buffer (as above with 0.5% NP-40) and collected. The beads were then subjected to RNA or protein extraction as described later.

2.8. Chromatin IP

Chromatin IP (ChIP) was performed as per Cotney and Noonan's protocol (Cotney and Noonan, 2015).

2.9. Chromatin isolation by RNA purification (ChIRP)

ChIRP was carried out according to the protocol of Chu et al. (2012). Oligo sequences are provided in Supplementary Table 7.

2.10. RNA isolation and PCR

Total RNA was isolated from cells or tissues using TRIzol (Thermo Fisher Scientific) for RNA-sequencing and IP or using RNAiso Plus (Takara Bio) for analysis by qRT-PCR as per the manufacturer's protocol. Real-time PCR was performed using SyBr green mix (Takara) in real-time PCR machine (BioRad CFX96). All primer sequences have been provided in Supplementary Table 8.

2.11. RNA-Seq analysis

E14TG2a cells treated with scrambled or Mrhl shRNA (shRNA 4) were subjected to RNA isolation and quality check. RNA samples were then subjected to library preparation in duplicates and sequenced on Illumina Hi-Seq 2500 platform. RNA-Seq analysis was performed as described previously (Trapnell et al., 2012). The threshold for DE genes was log2 (fold change) >1.5 for up regulated genes and log2 (fold change) <1.5 for down regulated genes. The DE genes were analyzed further using R CummeRbund package. Gene Ontology (GO) analysis was performed in PANTHER (Thomas et al., 2003). Fisher's exact test was performed in PANTHER Gene Ontology (GO).

2.12. Cluster analysis

Hierarchical clustering method was performed using Cluster 3.0 (de Hoon et al., 2004). Clusters were visualized as a network in Cytoscape (Shannon et al., 2003). Functional enrichment of each cluster was performed using the Gene Mania Tool (Warde-Farley et al., 2010).

2.13. TF network analysis

Motifs were downloaded for all transcription factors from JASPAR (Mathelier et al., 2014) and sequence of interest for each TF (1.5 kb upstream & 500 bp downstream of TSS) was extracted using BedtoFasta of the Bedtools suite (Quinlan and Hall, 2010). Then each motif was scanned across the sequence of all TFs to create the table matrix that reflects the number of binding sites for each TF across the other TFs using MEME suite (Bailey et al., 2009) with an e-value of 1E-04. Finally the heatmap was generated from the table matrix using R 3.3.2. TFs were fed into STRING (Jensen et al., 2009) to obtain the interaction

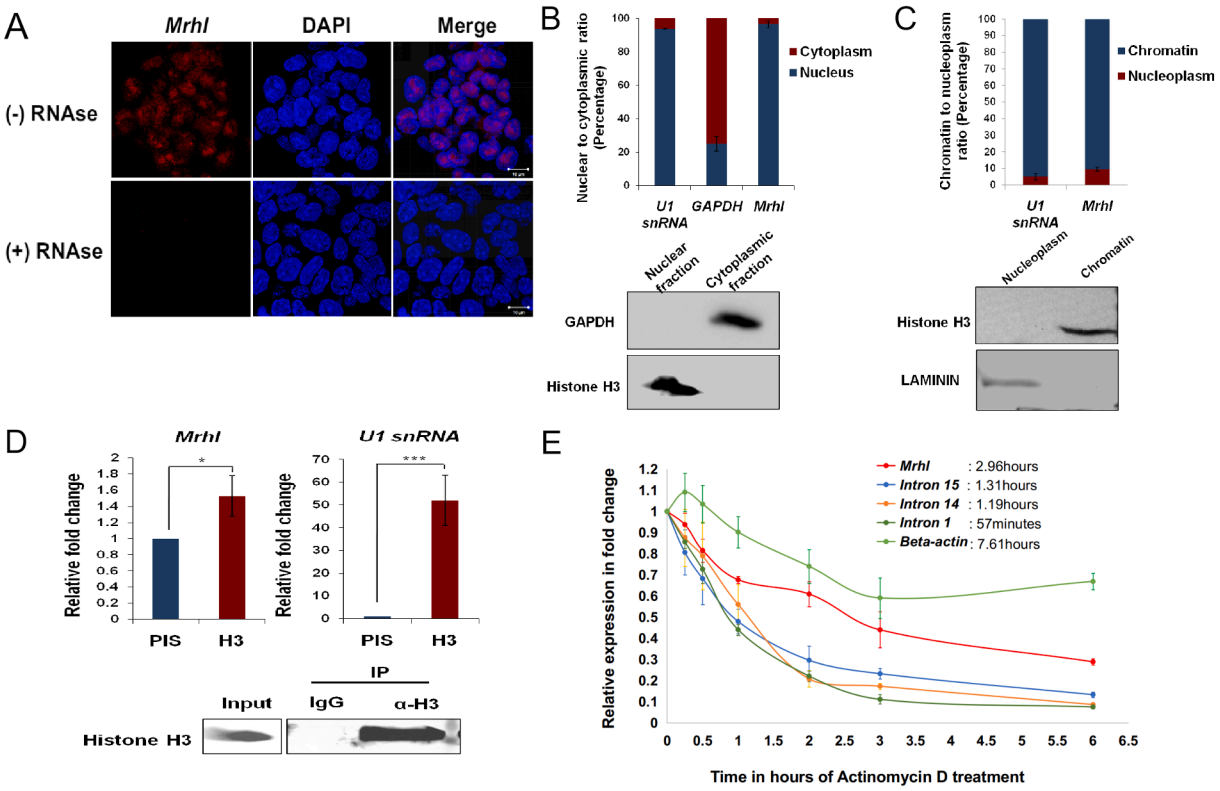

Fig. 1. Mrhl is a nuclear-localized, chromatin bound moderately stable lncRNA in mESCs. (A) RNA FISH shows nuclear localization of Mrhl in mESCs; (B) Fractionation validated observations in panel A. Western blot shows purity of fractions; (C) Chromatin and nucleoplasm fractions of nuclei show localization of Mrhl to chromatin. Western blot shows purity of fractions; (D) H3 ChIP and qPCR reveal Mrhl is bound with the chromatin in mESCs; (E) Actinomycin D half-life assay for Mrhland Phkb introns in mESCs. Error bars indicate standard deviation from three independent experiments. *p < 0.05, **p < 0.01, ***p < 0.001, student's *t*-test; Scale bar = 10 μm.

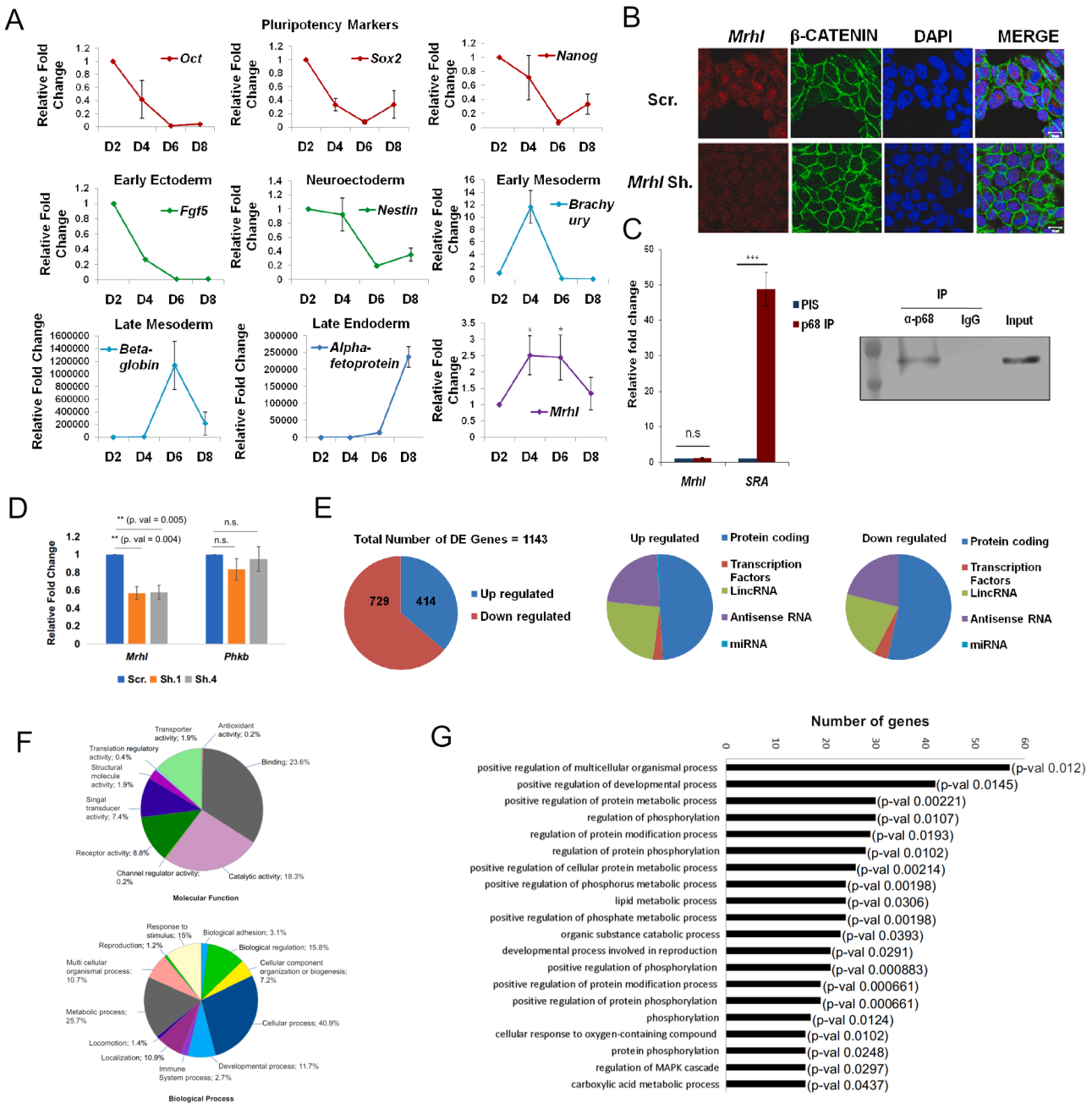

Fig. 2. Mrhl regulates development and differentiation related processes in mESCs. (A) Mrhl shows differential expression during EB differentiation of mESCs; (B, C) Mrhl does not function through the WNT/p68 cascade unlike in spermatogonial progenitors; (D) Knockdown efficiency of Mrhl in mESCs and corresponding Phkb levels through two independent constructs i.e. sh.1 and sh.4 as compared to scrambled (scr.) control; (E) Representation of DEG classification; (F) Gene ontology analysis of DEG; (G) GO enrichment analysis of DEG. Error bars indicate standard deviation from three independent experiments. *p < 0.05, **p < 0.01, ***p < 0.001, student's *t*-test; Scale bar = 10 μm.

among given TFs (proteins).

2.14. ChIRP-Seq analysis

mm10 Genome was downloaded from GENCODE and indexed using Bowtie2-build with default parameters. Adapter trimming was done using Trim Galore (v 0.4.4) and each of the raw Fastq files were passed through a quality check using the FastQC. PCR duplicates were removed using the Samtools 1.3.1 with the help of 'rmdup' option. Each of the raw files was then aligned to mm10 genome assembly using Bowtie 2 with default parameters for paired-end sequencing. As per principal component analysis, the correlation coefficient for the replicate samples for ChIRP/treated was 0.8 whereas that for the input samples was 0.65. Replicates of both control and treated were merged respectively. Peaks were called using MACS2. Final peaks were selected giving the criteria of above 5-fold change and p value <0.05. Motifs were identified using MEME, using the criteria of One Occurrence Per Sequence (OOPS) and significance of 1E-04 for 21,282 genomic loci.

2.15. Triplex prediction

Sequence from the Mrhl occupied region (in addition extended upto +/- 25 bp) of selected genes was used for Triplex prediction using the software Triplexator (Buske et al., 2012) with default parameters.

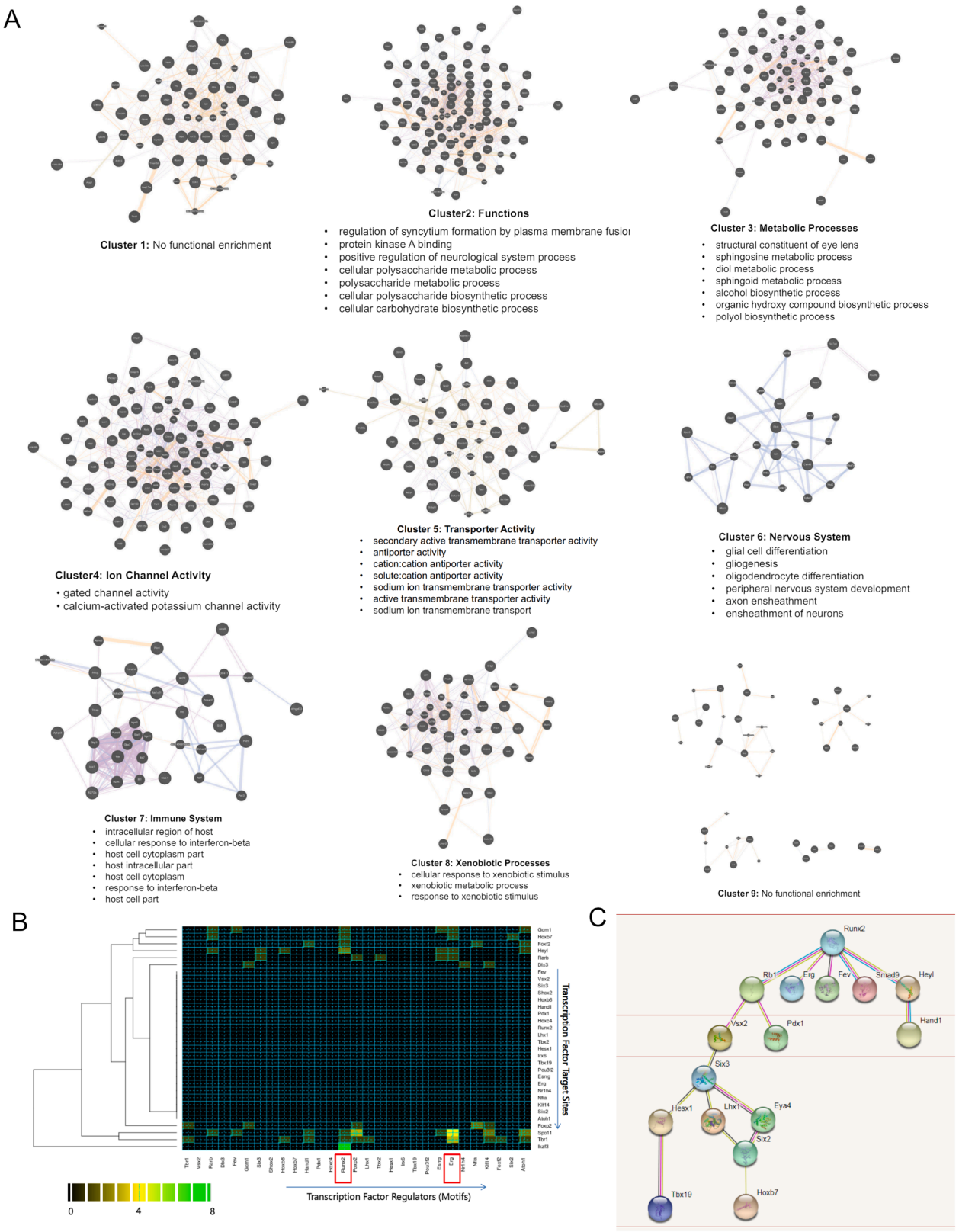

Fig. 3. Gene co-expression and TF network analyses. (A) Gene co-expression modules and their corresponding functional enrichments. Each edge represents how heavily weighted are the paths between the nodes; (B) Heat map visualization of TF matrix; (C) TF hierarchy as visualized in STRING.

3. Results

3.1. Mrhl is a nuclear-localized, chromatin bound moderately stable lncRNA in mESCs

We analyzed poly (A) RNA-Seq datasets from the ENCODE database and observed that Mrhl is expressed predominantly in the embryonic stages of tissues of various lineages (Suppl. Fig. 1) with expression being almost nil in the postnatal stages. From E8.5 onwards, the mouse embryo undergoes a surge of differentiation, cell specification and organogenesis phenomena. Our data analysis suggested that Mrhl might have a selective role to play in these processes in the context of mouse embryonic development. To address this, we used mESCs as our model system of study. RNA FISH revealed Mrhl to be expressed primarily in the nulcei of mESCs (Fig. 1A). Biochemical fractionation further validated Mrhl to be present in the nuclear fraction, specifically the chromatin fraction in mESCs (Fig. 1B, C). We next addressed if Mrhl is associated with the chromatin for which we performed H3 ChIP and we observed significant enrichment of Mrhl in H3 bound chromatin (Fig. 1D). Since Mrhl is located within the intron 15 of the Phkb gene and transcribed in the same orientation, we wanted to discern if the RNA-FISH signals are arising from the nascent transcript of Mrhl or from the pre-mRNA of Phkb. We would expect that other introns of the pre-mRNA of Phkb would exhibit much lower stability than Mrhl, since Mrhl is independently transcribed. For this purpose, we performed an assay for RNA half-life for *Phkb* introns 1, 14 and another region from intron 15. Indeed we found Mrhl to display ~2.5 times more stability with a half-life of 2.96 h in mESCs, in comparison to the other intronic regions (Fig. 1E), suggesting RNA FISH signals are of the nascent Mrhl transcript. Our observations herewith prompted us to investigate further the functional relevance of Mrhl in mESCs.

3.2. Mrhl regulates development and differentiation circuits in mESCs

We next differentiated the mESCs into embryoid bodies (EBs) and interestingly observed that Mrhl was preferentially up regulated at days 4 and 6 of EB formation (Fig. 2A). In perspective of the negative feedback regulation between Mrhl and WNT signaling in spermatogonial progenitors and of WNT signaling contributing to mESC physiology (Atlasi et al., 2013; Price et al., 2013; Sokol, 2011), we questioned whether Mrhl would function through similar mechanisms in this context as well. We performed shRNA mediated knockdown of Mrhl in mESCs and scored for its levels using RNA FISH followed by the status of β-CATENIN localization by IF. We observed that in cells where Mrhl was depleted with high efficiency, β-CATENIN was still localized at the membrane indicating non-activation of the WNT pathway (Fig. 2B). This was further validated by observing the expression of WNT pathway targets *Axin2* and *c-Myc* wherein they did not show any changes in their levels (Suppl. Fig. 2A). Furthermore, p68 IP revealed that Mrhl does not interact with p68 in mESCs (Fig. 2C). Keeping these observations in mind, we performed transient knockdown of Mrhl in mESCs using four independent constructs, two of which (referred to as sh. 1 and sh. 4 henceforth) showed us an average down regulation of 50% with no impact on the abundance of the host transcript *Phkb* (Fig. 2D). We then subjected the scrambled (scr.) and sh.4 treated cells to analysis by RNA-Seq. A quick comparison of the FPKM values for Mrhl obtained in our analysis versus those reported in the ENCODE database displayed Mrhl to be a low abundant lncRNA in mESCs along with confirming our knockdown efficiency (Suppl. Fig. 2B). Furthermore, we observed that the expression of pluripotency genes *Oct4*, *Sox2* and *Nanog* were not affected upon Mrhl knockdown in mESCs (Suppl. Fig. 2C). We also observed from the RNA-Seq data that the fold change for Phkb in Mrhl knockdown condition was only −0.03 (data not shown), confirming no significant perturbation in the levels of host Phkb transcript. We obtained a total of 1143 genes which were dysregulated in expression with 729 being down regulated and 414 being up regulated in expression (Fig. 2E) and we refer to them as the differentially expressed genes (DEG, Supplementary File 1). Gene ontology (GO) analysis of the DEGusing *Mus musculus* whole genome revealed diverse molecular functions such as binding (23.6%), catalytic activity (18.3%), receptor activity (8.8%) and signal transducer activity (7.4%) and biological processes such as cellular processes (40.9%), biological regulation (15.8%), metabolic process (25.7%), developmental process (11.7%) and multicellular organismal process (10.7%) to be affected (Fig. 2F). We next performed a GO enrichment analysis with a p-value <0.05 and Bonferroni correction to understand if one or more of the perturbed processes/pathways were statistically over represented over the others and we found positive regulation of developmental processes and positive regulation of multicellular organismal processes to be two such enriched perturbed processes (Fig. 2G). To further narrow down, we performed Fisher's exact test in the PANTHER interface with a p-value <0.001 and obtained several interesting GO categories to be further enriched (Suppl. Table 1) with the category of developmental processes (GO:0032502, Supplementary File 2) posing as the most interesting one since it appeared in both the enrichment analyses and possessed the maximum number of perturbed genes i.e., 60 with a significant p-value of 6.44E−05. We examined the DEG belonging to this category and found that they belonged to two broad groups of lineage-specific TFs and cell adhesion/receptor activity related genes. The former group comprised genes encoding factors involved in neuronal lineage, hematopoietic and vascular lineage, cardiac lineage, skeletal lineage, mesodermal lineage and pancreatic lineage (Suppl. Table 2) whereas the latter group consisted of genes responsible for such functions as migration, axon guidance, signaling, growth and differentiation, structural roles and cellular proliferation amongst others (Suppl. Table 3). From our assays and analyses herewith, we conclude that Mrhl majorly acts to regulate differentiation and development related genes and processes in mESCs. Also, we compared the DEG in Mrhl knockdown conditions in mESCs and GC1-Spg spermatogonial progenitors and made two observations: firstly, the perturbed transcriptome is vastly different, emphasizing the context-dependent role of Mrhl and secondly, about 25 genes were in common between the two datasets, suggesting some common target genes of regulation for Mrhl across developmental model systems (Suppl. Fig. 2D).

3.3. Gene co-expression and TF interaction analyses show unique networks to be coordinated by Mrhl in mESCs

In order to organize the perturbed transcriptome under conditions of Mrhl knockdown in mESCs into functional and biologically relevant modules (Chen et al., 2018, 2016), we performed hierarchical clustering of the DEG. Gene expression data (FPKM of all samples i.e., scrambled and shRNA treated) was taken and log2 transformed. Low expressed (FPKM $<$ 0.05) and invariant genes were removed. Then genes were centered and clustering was performed based on differential expression pattern of genes and fold change. We then visualized the resultant clusters or modules with Cytoscape (Fig. 3A). We obtained nine such co-expression modules with diverse functional enrichments such as ion channel and transporter activities for clusters 4 and 5, nervous system functions for cluster 6, immune system processes for cluster 7 and responses to xenobiotic stimuli for cluster 8. Clusters 2 and 3 had varied functional enrichments whilst clusters 1 and 9 did not show any of such functional representations. We also performed a TF-TF interaction analysis to understand the potential cross-talk between the dysregulated set of TFs (Supplementary File 3) and to identify a master TF through which Mrhl might be acting to regulate the TF network. TFs have been implicated often in determining cellular states or fates (Dunn et al., 2014; Goode et al., 2016). A gene ontology analysis of the perturbed TFs revealed metabolic processes and developmental processes to be over represented in function (Suppl. Fig. 3A). Subsequent construction of the TF matrix and TF hierarchy (Fig. 3B, C) revealed RUNX2 as a potential master TF since it had the maximum number of motifs for binding across

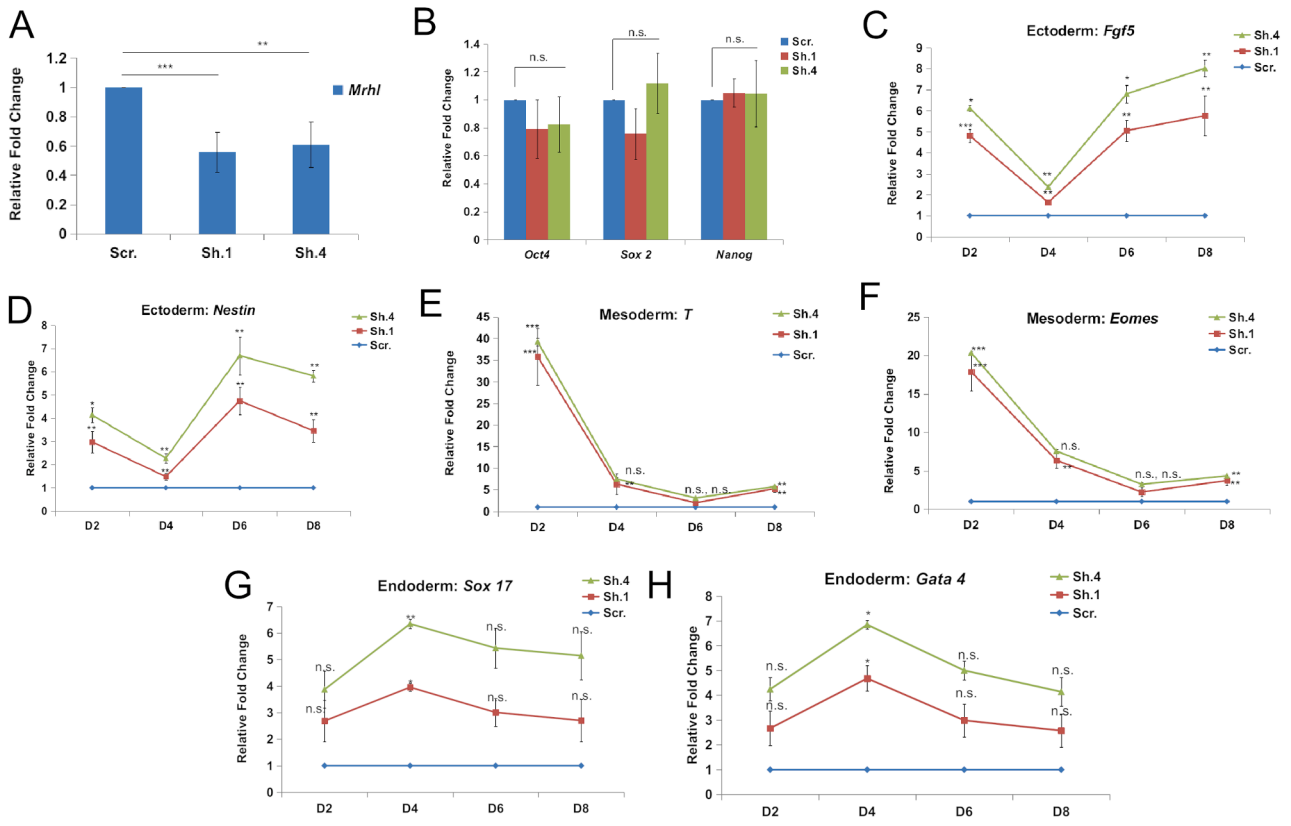

Fig. 4. Stable knockdown of Mrhl in mESCs causes no change in pluripotency status but aberrance in lineage specification. (A) Knockdown efficiency in puromycin selected stable knockdown cells; (B) qRT-PCR for pluripotency markers; (C–H) qRT-PCR for lineage-specific markers upon EB differentiation of stable knockdown cells as compared to scrambled control. Error bars indicate standard deviation from three independent experiments. *p < 0.05, **p < 0.01, ***p < 0.001, student's *t*-test; Panel C-Hare representative data from one of three independent experiments, each carried out in biological triplicates.

the promoters of all the other TFs (Suppl. Fig. 3B). Thus, we report a novel TF network or hierarchy operating in mESCs in the context of Mrhl. Furthermore, since many of the gene co-expression clusters and TFs are related to developmental phenomena or processes, the analyses herewith further emphasize on Mrhl acting to control cell fate specification and differentiation related circuits in mESCs.

3.4. Stable knockdown of Mrhl in mESCs shows aberrance in lineage specification

Towards understanding the phenotypic implications of Mrhl depletion in mESCs and of our transcriptome analyses, we generated stable knockdown lines for Mrhlsh.1, sh.4 and scr. control. Our initial characterization of the stable knockdown cells showed a knockdown efficiency of 40–50% (Fig. 4A) with no discernible change in the pluripotency markers *Oct4*, *Sox2* and *Nanog* (Fig. 4B) in the knockdown versus control lines. Keeping in mind our earlier conclusions from the transcriptome analyses and the observation that Mrhl is up regulated in expression during EB differentiation, we subjected the knockdown and control cells to EB differentiation. Interestingly, we observed that over days 2 to 8 of differentiation, there was a marked aberrance in the specification of lineages. For the ectoderm lineage, there appeared to be an overall increase in the expression levels of the corresponding markers*Fgf5* and *Nestin* (Fig. 4C, D) whereas the mesoderm lineage appeared to exhibit premature specification at day 2 with subsequent loss of lineage maintenance at days 4 to 8 of differentiation (Fig. 4E, F). For the endoderm lineage, all markers were up regulated at all time points in knockdown cells as compared to control by >2-fold. (Fig. 4G, H). These observations suggest that knockdown of Mrhl in mESCs causes a skew in the specification of early lineages during their differentiation, implying that Mrhl is required in mESCs to undergo a balanced differentiation module, although it might not have a specific role in mESCs per se in the absence of differentiation cues.

3.5. Mrhl regulates target loci in mESCs through chromatin-mediated regulation

In order to further delineate the mechanism by which Mrhl regulates differentiation and developmental pathways in mESCs, we performed genome-wide chromatin occupancy studies through ChIRP-Seq since we have demonstrated Mrhl to be a chromatin bound lncRNA in mESCs. Mrhl bound chromatin was pulled down with high efficiency (Suppl. Fig. 4A) and subjected to sequencing. We obtained a total of 21,997 raw peaks and after keeping a cutoff value of 5-fold enrichment, we obtained 21,282 peaks (Fig. 5A, Supplementary File 4), indicating widespread chromatin occupancy of Mrhl in mESCs. The peak lengths and fold changes were distributed equally across all the chromosomes (Suppl. Fig. 4B, C). An annotation of the enriched peaks showed us that diverse regions including intronic, intergenic and promoter regions of genes as well as repeat elements undergo physical association with Mrhl (Fig. 5B). Next, we overlapped the peaks from ChIRP-Seq and the DEG from RNA-Seq to understand what proportion of the dysregulated genes upon Mrhl knockdown is regulated by it at the chromatin level. In this regard, we have used −10 kb upstream of transcription start site (TSS) and +5 kb downstream of TSS of genes as our domain of target gene regulation by Mrhl which narrowed down the number of peaks to 3412. The overlap analysis revealed 71 genes which are physically occupied and are also regulated by Mrhl at the chromatin level (Fig. 5C, Supplementary File 5). We further examined the 71 genes in detail and found a subset of six genes i.e., *Runx2*, *Six2*, *Dlx3*, *Hoxb7*, *Pou3f2* and *Foxp2* to be of noticeable importance in terms of being lineage determining or development associated transcription factors (Suppl. Table 4).

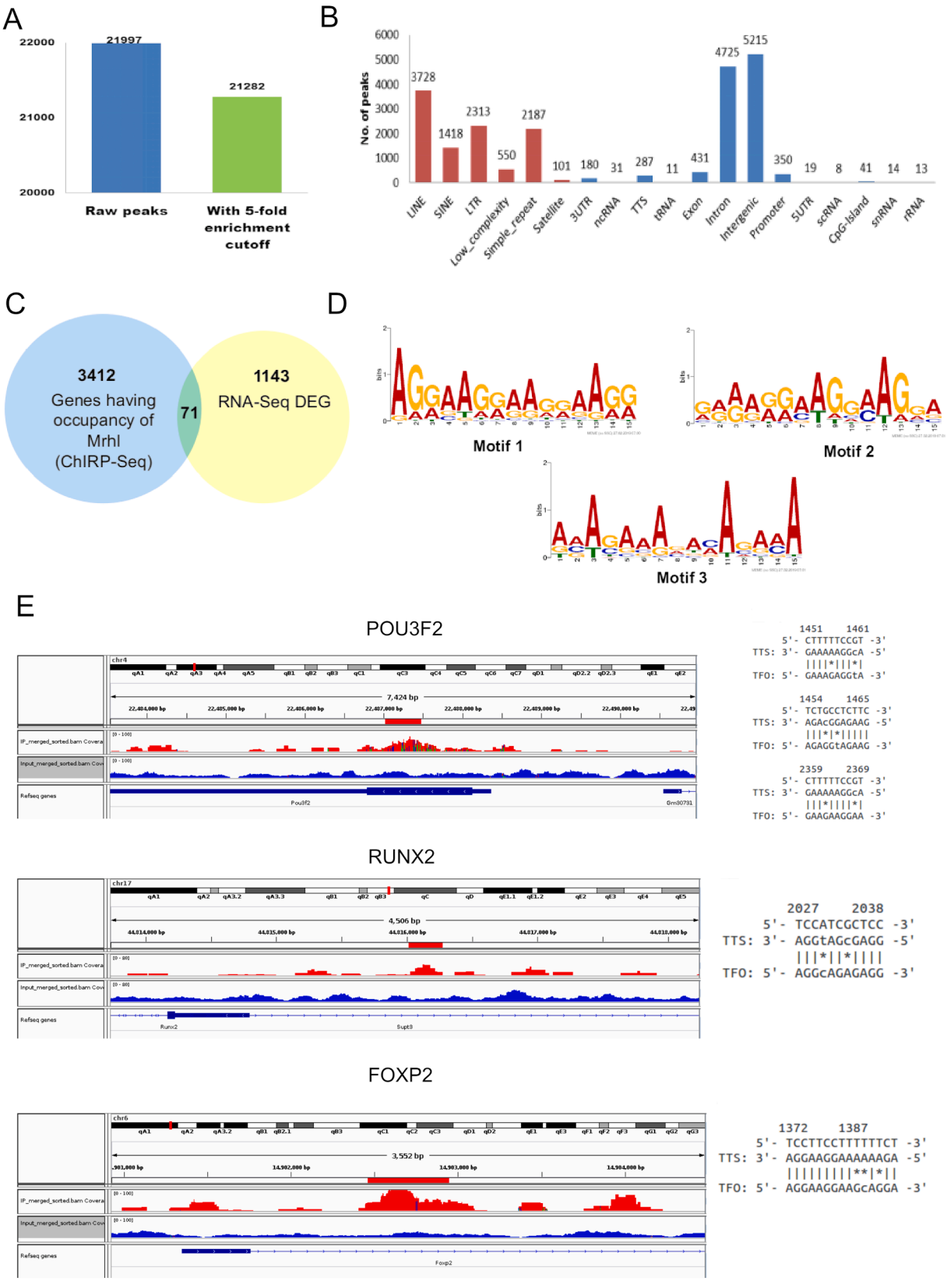

Fig. 5. ChIRP-Seq analysis for Mrhl in mESCs. (A) Number of peaks obtained before and after cutoff; (B) Annotation of peaks; (C) Overlap of ChIRP-Seq and RNA-Seq datasets; (D) Motif analysis for genome occupancy for Mrhl on target genes; (E) Triplex formation prediction at select loci involved in development and differentiation functions. Tracks in red are for pulldown and tracks in blue are for input. TFO: Triplex Forming Oligonucleotide, TTS: Triplex Target Site. (For interpretation of the references to colour in this figure legend, the reader is referred to the web version of this article.)

A recently established mechanism of chromatin-mediated target gene regulation by lncRNAs is via the formation of RNA-DNA-DNA triple helical structures (Mondal et al., 2015; Postepska-Igielska et al., 2015; Wang et al., 2018) and hence we hypothesized triplex formation by Mrhl at target loci. We performed this analysis on a fewcandidate genes i.e., *Runx2*, *Hoxb7*, *Foxp2* and *Pou3f2*. Their roles in governing the development of specific lineages such as the osteoblast lineage [*Runx2*RUNX2 (Komori, 2002)], neuronal lineage and brain development [*Foxp2* (Chiu et al., 2014; Tsui et al., 2013), *Pou3f2* (Lin et al., 2018; Urban et al., 2015)) or having multiple functions during development [*Hoxb7*(Candini et al., 2015; Klein et al., 2013)] have been widely established. A search for sequence motifs for Mrhl binding to target chromatin loci led to the identification of three distinct motifs with motif 1 being present in 21.46%, motif 2 being present in 28.16% and motif 3 being present in 43.08% of the total number of peaks. (Fig. 5D and Suppl. Table 5). Next, triplex formation analysis was studied using the sequence of Mrhl +/− 25 bp as the triplex forming oligonulceotide (TFO) and the Mrhl occupied region on the target gene, as inferred from our ChIRP-Seq data, as the triplex target site (TTS). We observed the presence of only one motif (motif 3) at the Mrhl occupied region in *Pou3f2*, motifs 1, 2 and 3 in *Foxp2* and again motif 3 in *Runx2* and *Hoxb7*. Interestingly, for *Pou3f2*, triplex forming potential was present at two different sites with one lying within the motif sequence whereas in *Foxp2* and *Runx2*2, potential triplex forming sites were found immediately adjacent to the motif sequences. *Hoxb7*, however, did not show propensity for triplex formation within the Mrhl occupied region (Fig. 5E, Suppl. Table 6, upplementary File 6). In lieu of these observations, we conclude that Mrhl regulates key lineage-specific TFs at the chromatin possibly through triple helix formation to regulate differentiation of mESCs.

4. Discussion

The extensive context-dependent roles of lncRNAs in ESC physiology pose them as novel therapeutic targets in the context of regenerative medicine. Linc-RoR mediates the formation of human induced pluripotent stem cells (Loewer et al., 2010) and contributes to human embryonic stem cell self-renewal (Wang et al., 2013) whereas lncRNA Cyrano is involved in maintenance of pluripotency of mESCs (Smith et al., 2017). In parallel, linc-RoR has been implicated in osteogenic differentiation of mesenchymal stem cells (Feng et al., 2018) whilst Cyrano has been shown to function in conjunction with other non-coding RNAs to regulate neuronal activity in the mammalian brain (Kleaveland et al., 2018) as well as neurodevelopment in zebrafish (Sarangdhar et al., 2018). In our current study, we show that lncRNA Mrhl depletion majorly dysregulates pathways and processes in mESCs which are related to lineage-specific development and differentiation and which are largely distinct from the perturbed gene set in spermatogonial progenitors. This emphasizes the context-dependant role of Mrhl as a molecular player of the cellular system. A lack of perturbation of pluripotency status of mESCs upon Mrhl knockdown in combination with aberrance in lineage specification, suggest Mrhl to be involved in specifying a primed state of the mESCs wherein they can undergo balanced specification of lineages upon obtaining differentiation cues. Furthermore, in our ENCODE data analysis of organs, Mrhl was observed to be expressed predominantly in embryonic stages of organs of various lineages such as the brain (ectoderm), kidney, testes (mesoderm) and lung, liver (endoderm). An interrogation of Mrhl expression in the recently released Mouse Organogenesis Cell Atlas (Cao et al., 2019) showed Mrhl to be expressed in progenitor cell types of various tissues (data not shown). This can only give us a preliminary insight about the involvement of Mrhl not only in the early stages of germ layer specification but in the later stages of organogenesis as well, although the exact functions in the latter need to be still addressed. Other disrupted pathways such as ion transport which have been recurrent in all systems analyses would be an interesting aspect to address in the future. It would also be interesting to address the protein interaction partners of Mrhl in mESCs, especially to understand in greater depth how Mrhl mediates regulation at target genes.

The regulation of a novel TF network in mESCs by Mrhl comprising mostly lineage-determining TFs is a significant observation. TFs act to govern gene expression programs defining particular cellular states, more so in association with other TFs in a network (Dore and Crispino, 2011; Niwa, 2018). LncRNAs often integrate into such networks by regulating TFs individually or via a master TF(s) resulting in downstream regulation of gene expression (Herriges et al., 2014; Yo and Runger, 2018). The TF network operating in mESCs under the regulation of Mrhl has RUNX2 at the top of the hierarchy posing it as a master TF in the hierarchy and being potentially regulated by Mrhl directly through triplex formation at the chromatin level. The role of nuclear lncRNAs in coordinating and controlling gene expression at a genome-wide level through the regulation of chromatin architecture/chromatin state at target loci is well known (Ballarino et al., 2018; Cajigas et al., 2015; Sun et al., 2018a). The absence of triplex formation sites in HOXB7 in spite of the presence of Mrhl binding motifs in its promoter further strengthens the hypothesis that Mrhl might be regulating the entire network through RUNX2. Additionally, FOXP2 and POU3F2 although not a part of the TF network, display triplex forming potential within the Mrhl occupied regions. These observations imply a mechanism wherein Mrhl regulates differentiation programs in mESCs through possible direct chromatin mediated regulation of relevant TFs.

A further analysis of our transcriptome studies herewith showed a significant over representation of dysregulated genes and processes belonging to neuronal lineage. Ectoderm development was one of the enriched processes in the Fisher's exact test and ~20% of the dysregulated genes in GO: 0032502 belonged to neuronal lineage development related functions. In the gene co-expression analysis, nervous system emerged as one of the perturbed clusters. Furthermore, Mrhl is predicted to regulate important neuronal TFs such as POU3F2 and FOXP2 directly at the chromatin level. Whilst our phenotype analysis of the stable knockdown cells showed perturbations in early specification of the ectoderm and mesoderm lineages, further investigations of the role of Mrhl in specifying more specialized lineages such as the neuronal lineage would be an interesting aspect of study.

LncRNAs have been implicated widely for their contributions to embryonic stem cell differentiation, cell fate specification, organogenesis and development through a diverse array of mechanisms (Grote and Herrmann, 2015; Perry and Ulitsky, 2016; Sarropoulos et al., 2019). In our studies we have characterized lncRNA Mrhl and its functional significance in mESC towards decoding its role in development. We show Mrhl to regulate downstream genes and processes involved in differentiation and lineage specification that was reflected in our phenotype studies. A major finding of this study was its potential direct chromatin mediated regulation of key TFs that mediate differentiation of stem cells into a specific lineage. Overall, we establish lncRNA Mrhl to be a mediator of differentiation and cell fate specification events in mESCs.

CRediT authorship contribution statement

Debosree Pal: Conceptualization, Methodology, Investigation, Data curation, Writing - original draft, Visualization. **C.V. Neha:** Methodology, Investigation. **Utsa Bhaduri:** Software, Formal analysis, Investigation, Data curation. **Zenia Zenia:** Methodology, Investigation. **Sangeeta Dutta:** Methodology, Validation, Investigation. **Subbulakshmi Chidambaram:** Methodology, Investigation. **M.R.S. Rao:** Conceptualization, Methodology, Writing - review & editing, Visualization, Supervision, Project administration, Funding acquisition.

Declaration of Competing Interest

The authors declare that they have no known competing financial interests or personal relationships that could have appeared to influence the work reported in this paper.

Acknowledgements

We thank Prof. Tapas Kumar Kundu (JNCASR, India) for providing E14TG2a mESCs and Prof. Maneesha Inamdar (JNCASR, India) for intellectual discussions. We thank Suma B.S. of the Confocal Imaging Facility, Dr. R.G. Prakash of the Animal Facility and Anitha G. of the Sequencing Facility at JNCASR, India. We thank Dhanur P. Iyer for initial help in standardization of RNA FISH technique. MRS Rao acknowledges Department of Science and technology, Govt of India for SERB Distinguished Fellowship and SERB-YOS (Year of Science Chair Professorship)and this work was financially supported by Department of Biotechnology, Govt. of India (Grant Numbers: BT/01/COE/07/09 and DBT/INF/22/SP27679/2018). Debosree Pal thanks University Grants Commission and JNCASR, India for her PhD fellowship. Sangeeta Dutta thanks Department of Biotechnology, Govt. of India for her postdoctoral fellowship. We thank the reviewers for their insightful comments and responses.

Deposited data

RNA-Seq and ChIRP-Seq datasets have been submitted to NCBI. The RNA-Seq dataset is available under accession number GSE159757.

Author contributions

D.P, N.CV, Z., S.C and S.D performed the experiments. D.P. and M.R. S designed the experiments and wrote the manuscript. U.B performed the computational data analysis associated with RNA-Seq and ChIRP-Seq. All authors approved the final manuscript.

Appendix A. Supplementary data

Supplementary data to this article can be found online at https://doi.org/10.1016/j.scr.2021.102250.

References

Akhade, V.S., Dighe, S.N., Kataruka, S., Rao, M.R., 2016. Mechanism of Wnt signaling induced down regulation of Mrhl long non-coding RNA in mouse spermatogonial cells. Nucleic Acids Res. 44 (1), 387–401. https://doi.org/10.1093/nar/gkv1023.

Akhade, V.S., Pal, D., Kanduri, C., 2017. Long noncoding RNA: genome organization and mechanism of action. Adv. Exp. Med. Biol. 1008, 47–74. https://doi.org/10.1007/978-981-10-5203-3_2.

Anguera, M.C., Ma, W., Clift, D., Namekawa, S., Kelleher 3rd, R.J., Lee, J.T., 2011. Tsx produces a long noncoding RNA and has general functions in the germline, stem cells, and brain. PLoS Genet. 7 (9) https://doi.org/10.1371/journal.pgen.1002248.

Arun, G., Akhade, V.S., Donakonda, S., Rao, M.R.S., 2012. mrhl RNA, a long noncoding RNA, negatively regulates Wnt signaling through its protein partner Ddx5/p68 in mouse spermatogonial cells. Mol. Cell. Biol. 32 (15), 3140–3152. https://doi.org/10.1128/MCB.00006-12.

Atlasi, Y., Noori, R., Gaspar, C., Franken, P., Sacchetti, A., Rafati, H., et al., 2013. Wnt signaling regulates the lineage differentiation potential of mouse embryonic stem cells through Tcf3 down-regulation. PLoS Genet. 9 (5) https://doi.org/10.1371/journal.pgen.1003424.

Bailey, T.L., Boden, M., Buske, F.A., Frith, M., Grant, C.E., Clementi, L., Ren, J., Li, W.W., et al., 2009. MEME SUITE: tools for motif discovery and searching. Nucleic Acids Res. 37 (Web Server), W202–W208. https://doi.org/10.1093/nar/gkp335.

Ballarino, M., Cipriano, A., Tita, R., Santini, T., Desideri, F., Morlando, M., et al., 2018. Deficiency in the nuclear long noncoding RNA Charme causes myogenic defects and heart remodeling in mice. EMBO J. 37 (18) https://doi.org/10.15252/embj.201899697.

Bergmann, J.H., Li, J., Eckersley-Maslin, M.A., Rigo, F., Freier, S.M., Spector, D.L., 2015. Regulation of the ESC transcriptome by nuclear long noncoding RNAs. Genome Res. 25 (9), 1336–1346. https://doi.org/10.1101/gr.189027.114.

Buske, F.A., Bauer, D.C., Mattick, J.S., Bailey, T.L., 2012. Triplexator: detecting nucleic acid triple helices in genomic and transcriptomic data. Genome Res. 22 (7), 1372–1381. https://doi.org/10.1101/gr.130237.111.

Cajigas, I., Leib, D.E., Cochrane, J., Luo, H., Swyter, K.R., Chen, S., et al., 2015. Evf2 lncRNA/BRG1/DLX1 interactions reveal RNA-dependent inhibition of chromatin remodeling. Development 142 (15), 2641–2652. https://doi.org/10.1242/dev.126318.

Candini, O., Spano, C., Murgia, A., Grisendi, G., Veronesi, E., Piccinno, M.S., Ferracin, M., Negrini, M., Giacobbi, F., Bambi, F., Horwitz, E.M., Conte, P., Paolucci, P., et al., 2015. Mesenchymal progenitors aging highlights a miR-196 switch targeting HOXB7 as master regulator of proliferation and osteogenesis: HOXB7 drives osteoprogenitors performance. Stem Cells 33 (3), 939–950. https://doi.org/10.1002/stem.1897.

Cao, J., Spielmann, M., Qiu, X., Huang, X., Ibrahim, D.M., Hill, A.J., Zhang, F., Mundlos, S., Christiansen, L., Steemers, F.J., Trapnell, C., et al., 2019. The single-cell transcriptional landscape of mammalian organogenesis. Nature 566 (7745), 496–502. https://doi.org/10.1038/s41586-019-0969-x.

Chakraborty, D., Paszkowski-Rogacz, M., Berger, N., Ding, L.i., Mircetic, J., Fu, J., Iesmantavicius, V., Choudhary, C., Anastassiadis, K., Stewart, A.F., et al., 2017. lncRNA Panct1 maintains mouse embryonic stem cell identity by regulating TOBF1 recruitment to Oct-Sox sequences in early G1. Cell Rep. 21 (11), 3012–3021. https://doi.org/10.1016/j.celrep.2017.11.045.

Chen, W., Zhang, X., Li, J., Huang, S., Xiang, S., Hu, X., Liu, C., 2018. Comprehensive analysis of coding-lncRNA gene co-expression network uncovers conserved functional lncRNAs in zebrafish. BMC Genomics 19 (Suppl. 2), 112. https://doi.org/10.1186/s12864-018-4458-7.

Chen, X., Liu, B., Yang, R., Guo, Y., Li, F., Wang, L., Hu, H., 2016. Integrated analysis of long non-coding RNAs in human colorectal cancer. Oncotarget 7 (17), 23897–23908. https://doi.org/10.18632/oncotarget.8192.

Chiu, Y.-C., Li, M.-Y., Liu, Y.-H., Ding, J.-Y., Yu, J.-Y., Wang, T.-W., 2014. Foxp2 regulates neuronal differentiation and neuronal subtype specification: Foxp2 regulates neuronal differentiation. Dev. Neurobiol. 74 (7), 723–738. https://doi.org/10.1002/dneu.22166.

Chu, C., Quinn, J., Chang, H.Y., 2012. Chromatin isolation by RNA purification (ChIRP). J. Vis. Exp. (61) https://doi.org/10.3791/3912.

Cotney, J.L., Noonan, J.P., 2015. Chromatin immunoprecipitation with fixed animal tissues and preparation for high-throughput sequencing. Cold Spring Harb. Protoc. 2015 (2), 191–199. https://doi.org/10.1101/pdb.prot084848.

de Hoon, M.J.L., Imoto, S., Nolan, J., Miyano, S., 2004. Open source clustering software. Bioinformatics 20 (9), 1453–1454. https://doi.org/10.1093/bioinformatics/bth078.

de Planell-Saguer, M., Rodicio, M.C., Mourelatos, Z., 2010. Rapid in situ codetection of noncoding RNAs and proteins in cells and formalin-fixed paraffin-embedded tissue sections without protease treatment. Nat. Protoc. 5 (6), 1061–1073. https://doi.org/10.1038/nprot.2010.62.

Dore, L.C., Crispino, J.D., 2011. Transcription factor networks in erythroid cell and megakaryocyte development. Blood 118 (2), 231–239. https://doi.org/10.1182/blood-2011-04-285981.

Dunn, S.-J., Martello, G., Yordanov, B., Emmott, S., Smith, A.G., 2014. Defining an essential transcription factor program for naive pluripotency. Science 344 (6188), 1156–1160. https://doi.org/10.1126/science:1248882.

Eisen, M., Imoto, S., Miyano, S., 1998. Cluster 3.0. Stanford, Stanford University.

Fatima, R., Choudhury, S.R., Divya, T.R., Bhaduri, U., Rao, M.R.S., 2019. A novel enhancer RNA, Hmrhl, positively regulates its host gene, phkb, in chronic myelogenous leukemia. Non-coding RNA Res. 4 (3), 96–108. https://doi.org/10.1016/j.ncrna.2019.08.001.

Feng, L.u., Shi, L., Lu, Y.-F., Wang, B., Tang, T., Fu, W.-M., He, W., Li, G., et al., 2018. Linc-ROR promotes osteogenic differentiation of mesenchymal stem cells by functioning as a competing endogenous RNA for miR-138 and miR-145. Mol. Ther. Nucleic Acids 11, 345–353. https://doi.org/10.1016/j.omtn.2018.03.004.

Flynn, R., Chang, H., 2014. Long noncoding RNAs in cell-fate programming and reprogramming. Cell Stem Cell 14 (6), 752–761. https://doi.org/10.1016/j.stem.2014.05.014.

Goff, L.A., Trapnell, C., Kelley, D., 2012. CummeRbund: visualization and exploration of Cufflinks high-throughput sequencing data. R package version 2 (0).

Goode, D.K., Obier, N., Vijayabaskar, M.S., Lie, A.L.M., Lilly, A.J., Hannah, R., et al., 2016. Dynamic gene regulatory networks drive hematopoietic specification and differentiation. Dev. Cell 36 (5), 572–587. https://doi.org/10.1016/j.devcel.2016.01.024.

Grote, P., Herrmann, B.G., 2015. Long noncoding RNAs in organogenesis: making the difference. Trends Genet. 31 (6), 329–335. https://doi.org/10.1016/j.tig.2015.02.002.

Guttman, M., Donaghey, J., Carey, B.W., Garber, M., Grenier, J.K., Munson, G., et al., 2011. lincRNAs act in the circuitry controlling pluripotency and differentiation. Nature 477 (7364), 295–300. https://doi.org/10.1038/nature10398.

Herriges, M.J., Swarr, D.T., Morley, M.P., Rathi, K.S., Peng, T., Stewart, K.M., Morrisey, E.E., 2014. Long noncoding RNAs are spatially correlated with transcription factors and regulate lung development. Genes Dev. 28 (12), 1363–1379. https://doi.org/10.1101/gad.238782.114.

Jensen, L.J., Kuhn, M., Stark, M., Chaffron, S., Creevey, C., Muller, J., et al., 2009. STRING 8–a global view on proteins and their functional interactions in 630 organisms. Nucleic Acids Res. 37 (Database), D412–D416. https://doi.org/10.1093/nar/gkn760.

Jin, C., Zheng, Y., Huang, Y., Liu, Y., Jia, L., Zhou, Y., 2017. Long non-coding RNA MIAT knockdown promotes osteogenic differentiation of human adipose-derived stem cells. Cell Biol. Int. 41 (1), 33–41. https://doi.org/10.1002/cbin.10697.

Klattenhoff, C., Scheuermann, J., Surface, L., Bradley, R., Fields, P., Steinhauser, M.L., et al., 2013. Braveheart, a long noncoding RNA required for cardiovascular lineage commitment. Cell 152 (3), 570–583. https://doi.org/10.1016/j.cell.2013.01.003.

Kleaveland, B., Shi, C.Y., Stefano, J., Bartel, D.P., 2018. A network of noncoding regulatory RNAs acts in the mammalian brain. Cell 174 (2), 350–362.e17. https://doi.org/10.1016/j.cell.2018.05.022.

Klein, D., Benchellal, M., Kleff, V., Jakob, H.G., Ergün, S., 2013. Hox genes are involved in vascular wall-resident multipotent stem cell differentiation into smooth muscle cells. Sci. Rep. 3, 2178. https://doi.org/10.1038/srep02178.

Komori, T., 2002. Runx2, A multifunctional transcription factor in skeletal development. J. Cell. Biochem. 87 (1), 1–8. https://doi.org/10.1002/jcb.10276.

Langmead, B., Salzberg, S.L., 2012. Fast gapped-read alignment with Bowtie 2. Nature methods 9 (4), 357.
Li, H., Handsaker, B., Wysoker, A., Fennell, T., Ruan, J., Homer, N., et al., 2009. The sequence alignment/map format and SAMtools. Bioinformatics 25 (16), 2078–2079.
Lin, N., Chang, K.-Y., Li, Z., Gates, K., Rana, Z., Dang, J., et al., 2014. An evolutionarily conserved long noncoding RNA TUNA controls pluripotency and neural lineage commitment. Mol. Cell 53 (6), 1005–1019. https://doi.org/10.1016/j.molcel.2014.01.021.
Lin, Y.J., Hsin, I.L., Sun, H.S., Lin, S., Lai, Y.L., Chen, H.Y., et al., 2018. NTF3 is a novel target gene of the transcription factor POU3F2 and is required for neuronal differentiation. Mol. Neurobiol. 55 (11), 8403–8413. https://doi.org/10.1007/s12035-018-0995-y.
Loewer, S., Cabili, M.N., Guttman, M., Loh, Y.-H., Thomas, K., Park, I.H., et al., 2010. Large intergenic non-coding RNA-RoR modulates reprogramming of human induced pluripotent stem cells. Nat. Genet. 42 (12), 1113–1117. https://doi.org/10.1038/ng.710.
Marchese, F.P., Raimondi, I., Huarte, M., 2017. The multidimensional mechanisms of long noncoding RNA function. Genome Biol. 18 (1), 206. https://doi.org/10.1186/s13059-017-1348-2.
Mathelier, A., Zhao, X., Zhang, A.W., Parcy, F., Worsley-Hunt, R., Arenillas, D.J., et al., 2014. JASPAR 2014: an extensively expanded and updated open-access database of transcription factor binding profiles. Nucleic Acids Res. 42 (Database isuue), D142–D147. https://doi.org/10.1093/nar/gkt997.
Mercer, T.R., Qureshi, I.A., Gokhan, S., Dinger, M.E., Li, G., Mattick, J.S., Mehler, M.F., 2010. Long noncoding RNAs in neuronal-glial fate specification and oligodendrocyte lineage maturation. BMC Neurosci 11, 14. https://doi.org/10.1186/1471-2202-11-14.
Mi, H., Muruganujan, A., Thomas, P.D., 2012. PANTHER in 2013: modeling the evolution of gene function, and other gene attributes, in the context of phylogenetic trees. Nucleic Acids Res. 41 (D1), D377–D386.
Mondal, T., Subhash, S., Vaid, R., Enroth, S., Uday, S., Reinius, B., et al., 2015. MEG3 long noncoding RNA regulates the TGF-beta pathway genes through formation of RNA-DNA triplex structures. Nat. Commun. 6, 7743. https://doi.org/10.1038/ncomms8743.
Nishant, K.T., Ravishankar, H., Rao, M.R.S., 2004. Characterization of a mouse recombination hot spot locus encoding a novel non-protein-coding RNA. Mol. Cell Biol. 24 (12), 5620–5634. https://doi.org/10.1128/MCB.24.12.5620-5634.2004.
Niwa, H., 2018. The principles that govern transcription factor network functions in stem cells. Development 145 (6). https://doi.org/10.1242/dev.157420.
Perry, R.B., Ulitsky, I., 2016. The functions of long noncoding RNAs in development and stem cells. Development 143 (21), 3882–3894. https://doi.org/10.1242/dev.140962.
Pijnappel, W.P.A., Baltissen, M., Timmers, H.T.M., 2013. Protocol for Lentiviral Knock Down in Mouse ES Cells.
Postepska-Igielska, A., Giwojna, A., Gasri-Plotnitsky, L., Schmitt, N., Dold, A., Ginsberg, D., Grummt, I., 2015. LncRNA Khps1 regulates expression of the proto-oncogene SPHK1 via triplex-mediated changes in chromatin structure. Mol. Cell 60 (4), 626–636. https://doi.org/10.1016/j.molcel.2015.10.001.
Price, F.D., Yin, H., Jones, A., van Ijcken, W., Grosveld, F., Rudnicki, M.A., 2013. Canonical Wnt signaling induces a primitive endoderm metastable state in mouse embryonic stem cells. Stem Cells 31 (4), 752–764. https://doi.org/10.1002/stem.1321.
Quinlan, A.R., Hall, I.M., 2010. BEDTools: a flexible suite of utilities for comparing genomic features. Bioinformatics 26 (6), 841–842. https://doi.org/10.1093/bioinformatics/btq033.
Sandelin, Albin, Alkema, Wynand, Engström, Pär, Wasserman, Wyeth W., Lenhard, Boris, 2004. JASPAR: an open-access database for eukaryotic transcription factor binding profiles. Nucleic Acids Res. 32 (Suppl_1), D91–D94.
Sarangdhar, M.A., Chaubey, D., Srikakulam, N., Pillai, B., 2018. Parentally inherited long non-coding RNA Cyrano is involved in zebrafish neurodevelopment. Nucleic Acids Res. 46 (18), 9726–9735. https://doi.org/10.1093/nar/gky628.
Sarropoulos, I., Marin, R., Cardoso-Moreira, M., Kaessmann, H., 2019. Developmental dynamics of lncRNAs across mammalian organs and species. Nature 571 (7766), 510–514. https://doi.org/10.1038/s41586-019-1341-x.
Shannon, P., Markiel, A., Ozier, O., Baliga, N.S., Wang, J.T., Ramage, D., et al., 2003. Cytoscape: a software environment for integrated models of biomolecular interaction networks. Genome Res. 13 (11), 2498–2504. https://doi.org/10.1101/gr.1239303.
Sheik Mohamed, J., Gaughwin, P.M., Lim, B., Robson, P., Lipovich, L., 2010. Conserved long noncoding RNAs transcriptionally regulated by Oct4 and Nanog modulate pluripotency in mouse embryonic stem cells. RNA 16 (2), 324–337. https://doi.org/10.1261/rna.1441510.
Smith, K.N., Starmer, J., Miller, S.C., Sethupathy, P., Magnuson, T., 2017. Long noncoding RNA moderates microRNA activity to maintain self-renewal in embryonic stem cells. Stem Cell Rep. 9 (1), 108–121. https://doi.org/10.1016/j.stemcr.2017.05.005.
Sokol, S.Y., 2011. Maintaining embryonic stem cell pluripotency with Wnt signaling. Development 138 (20), 4341–4350. https://doi.org/10.1242/dev.066209.
Sun, Q., Hao, Q., Prasanth, K.V., 2018a. Nuclear long noncoding RNAs: key regulators of gene expression. Trends Genet. 34 (2), 142–157. https://doi.org/10.1016/j.tig.2017.11.005.
Sun, Z., Zhu, M., Lv, P., Cheng, L.u., Wang, Q., Tian, P., et al., 2018b. The long noncoding RNA Lncenc1 maintains naive states of mouse ESCs by promoting the glycolysis pathway. Stem Cell Rep. 11 (3), 741–755. https://doi.org/10.1016/j.stemcr.2018.08.001.
Szklarczyk, D., Franceschini, A., Wyder, S., Forslund, K., Heller, D., Huerta-Cepas, J., et al., 2015. STRING v10: protein–protein interaction networks, integrated over the tree of life. Nucleic Acids Res. 43 (D1), D447–D452.
Thomas, P.D., Campbell, M.J., Kejariwal, A., Mi, H., Karlak, B., Daverman, R., Narechania, A., 2003. PANTHER: a library of protein families and subfamilies indexed by function. Genome Res. 13 (9), 2129–2141. https://doi.org/10.1101/gr.772403.
Trapnell, C., Roberts, A., Goff, L., Pertea, G., Kim, D., Kelley, D.R., et al., 2012. Differential gene and transcript expression analysis of RNA-seq experiments with TopHat and Cufflinks. Nat. Protoc. 7 (3), 562–578. https://doi.org/10.1038/nprot.2012.016.
Tsui, D., Vessey, J.P., Tomita, H., Kaplan, D.R., Miller, F.D., 2013. FoxP2 regulates neurogenesis during embryonic cortical development. J. Neurosci. 33 (1), 244–258. https://doi.org/10.1523/JNEUROSCI.1665-12.2013.
Ulitsky, I., Shkumatava, A., Jan, C., Sive, H., Bartel, D., 2011. Conserved function of lincRNAs in vertebrate embryonic development despite rapid sequence evolution. Cell 147 (7), 1537–1550. https://doi.org/10.1016/j.cell.2011.11.055.
Urban, S., Kobi, D., Ennen, M., Langer, D., Le Gras, S., Ye, T., Davidson, I., 2015. A Brn2-Zic1 axis specifies the neuronal fate of retinoic-acid-treated embryonic stem cells. J. Cell Sci. 128 (13), 2303–2318. https://doi.org/10.1242/jcs.168849.
Wang, S., Ke, H., Zhang, H., Ma, Y., Ao, L., Zou, L., et al., 2018. LncRNA MIR100HG promotes cell proliferation in triple-negative breast cancer through triplex formation with p27 loci. Cell Death Dis. 9 (8) https://doi.org/10.1038/s41419-018-0869-2.
Wang, Y., Xu, Z., Jiang, J., Xu, C., Kang, J., Xiao, L., et al., 2013. Endogenous miRNA Sponge lincRNA-RoR regulates Oct4, Nanog, and Sox2 in human embryonic stem cell self-renewal. Dev. Cell 25 (1), 69–80. https://doi.org/10.1016/j.devcel.2013.03.002.
Warde-Farley, D., Donaldson, S.L., Comes, O., Zuberi, K., Badrawi, R., Chao, P., et al., 2010. The GeneMANIA prediction server: biological network integration for gene prioritization and predicting gene function. Nucleic Acids Res. 38 (Web Server issue), W214–W220. https://doi.org/10.1093/nar/gkq537.
Yo, K., Runger, T.M., 2018. The long non-coding RNA FLJ46906 binds to the transcription factors NF-kappaB and AP-1 and regulates expression of aging-associated genes. Aging (Albany NY) 10 (8), 2037–2050. https://doi.org/10.18632/aging.101528.